

Nondiffusive Brownian Motion Studied by Diffusing-Wave Spectroscopy

D. A. Weitz,⁽¹⁾ D. J. Pine,⁽²⁾ P. N. Pusey,⁽³⁾ and R. J. A. Tough⁽³⁾

⁽¹⁾*Exxon Research and Engineering Co., Route 22E, Annandale, New Jersey 08801*

⁽²⁾*Department of Physics, Haverford College, Haverford, Pennsylvania 19041*

⁽³⁾*Royal Signals and Radar Establishment, Malvern, Worcestershire WR14 3PS, United Kingdom*

(Received 10 May 1989)

On a short-time scale, Brownian particles undergo a transition from the initial ballistic trajectories to diffusive motion. Hydrodynamic interactions with the surrounding fluid lead to a complex time dependence of this transition. We directly probe this transition for colloidal particles by measuring the auto-correlation function of multiply scattered, transmitted light. We show that a quantitative interpretation is possible because the transport of the light is diffusive, resolving a conflict in previous measurements.

PACS numbers: 82.70.Kj, 05.40.+j, 42.20.Ji

The trajectory of a Brownian particle on time scales comparable to the viscous damping time reflects the intricate interplay between the short-range, random molecular forces and the long-range, hydrodynamic forces on the particle. For short times, the particle motion is "ballistic," while for long times, the motion is diffusive. The nature of the transition from ballistic to diffusive motion is determined by the interaction of the particle with the surrounding fluid.¹ The flow field, or vorticity, established in the fluid when the particle moves, reacts back on the Brownian particle, resulting in a persistence of the motion. This hydrodynamic memory is manifested as a "long-time tail" in the decay of the velocity auto-correlation function.² Thus, the nature of the short-time, nondiffusive, Brownian motion and the transition to diffusive trajectories are sensitive functions of the hydrodynamic interactions between a colloidal particle and the surrounding fluid. In this Letter, we use diffusing-wave spectroscopy (DWS), in which temporal correlations of multiply scattered light are analyzed,³⁻⁶ to probe the motion of Brownian particles at much shorter time and length scales than previously has been possible. Thus, we are able to explore the hydrodynamic memory effects which determine the behavior of the transition from ballistic to diffusive motion. Our data critically test available theories and suggest the need to include interparticle hydrodynamic interactions. Finally, we also resolve a current dispute concerning the fundamental mechanism of the transport of radiation in a multiply scattering medium.

Simple quantities describing the isotropic Brownian motion of a colloidal particle suspended in a liquid are

$\langle \Delta x^2(t) \rangle \equiv \langle [x(t) - x(0)]^2 \rangle$, one Cartesian component of its mean-square displacement, and the autocorrelation of its velocity, $R(t) \equiv \langle v_x(0)v_x(t) \rangle$; here the brackets indicate ensemble averages. These quantities are connected by the relation⁷

$$\langle \Delta x^2(\tau) \rangle = 2 \int_0^\tau (\tau - t) R(t) dt. \quad (1)$$

On a time scale short enough that $R(t) \approx R(0)$, Eq. (1) becomes $\lim_{\tau \rightarrow 0} \langle \Delta x^2(\tau) \rangle = R(0)\tau^2$. This result reflects the fact that the acceleration of any body must be finite so that its short-time motion is ballistic, its displacement changing linearly with time. At a time scale long compared to the decay of its velocity fluctuations the motion of a Brownian particle is a random-walk diffusion: Equation (1) becomes $\lim_{\tau \rightarrow \infty} \langle \Delta x^2(\tau) \rangle = 2D\tau$, where the particle's diffusion constant D is given by $D \equiv \int_0^\infty dt R(t)$. Clearly the nature of the transition from short-time ballistic to long-time diffusive motion is determined by the form of the velocity autocorrelation function $R(t)$. The simplest theory of Brownian motion predicts an exponential decay⁷ of $R(t)$ so that

$$\langle \Delta x^2(\tau) \rangle = 2D[\tau + T(e^{-\tau/T} - 1)], \quad (2)$$

where the decay time $T = m/6\pi\eta a$ is the ratio of the particle's mass to its friction coefficient; here η is the shear viscosity of the fluid and a the particle radius. However, this simple theory does not take proper account of the development in time of the vorticity in the liquid surrounding the moving particle, and a full hydrodynamic theory of Brownian motion yields a more complex form for $R(t)$ which, with use of Eq. (1), gives¹

$$\langle \Delta x^2(\tau) \rangle = 2D \left\{ \tau - 2 \left(\frac{\tau_v \tau}{\pi} \right)^{1/2} + \frac{2}{9} \tau_v \left(4 - \frac{\rho'}{\rho} \right) + \frac{3}{[\tau_v(5 - 8\rho'/\rho)]^{1/2}} \left[\frac{1}{\alpha_+^3} e^{\alpha_+^2 \tau} \operatorname{erfc}(\alpha_+ \sqrt{\tau}) - \frac{1}{\alpha_-^3} e^{\alpha_-^2 \tau} \operatorname{erfc}(\alpha_- \sqrt{\tau}) \right] \right\}, \quad (3)$$

where

$$\alpha_{\pm} = \frac{3}{2} \frac{3 \pm (5 - 8\rho'/\rho)^{1/2}}{\sqrt{\tau_v}(1 + 2\rho'/\rho)},$$

and ρ' and ρ are the densities of the particle and fluid. The time scale for diffusion of vorticity across a particle radius is $\tau_v = a^2\rho/\eta$ and is related to the friction time scale, $T = \frac{2}{9} \tau_v(\rho'/\rho)$.

Both Eqs. (2) and (3) exhibit the expected asymptotic behaviors: ballistic motion at short times, $\langle \Delta x^2(\tau) \rangle \propto \tau^2$, and diffusive motion at long times, $\langle \Delta x^2(\tau) \rangle \propto \tau$. However, the behavior of the transition between these two regimes is very different. In the first case it is exponential. By contrast, in the case of the hydrodynamic theory, the approach to the asymptotic diffusive regime is slow: The second ($\sqrt{\tau}$) term in Eq. (3) is less than 1% of the first only for $\tau \geq 10^4 \tau_v$, reflecting the effects of the $t^{-3/2}$ long-time tail in $R(t)$.

Brownian motion of suspended particles can be studied experimentally by dynamic light scattering (DLS), the analysis of temporal fluctuations in scattered laser light.⁷ To cause an appreciable decay in the measured time correlation function of the scattered intensity, a typical path traversed by a scattered photon must change by roughly one light wavelength, λ . This requires relatively large motion of the particles in the usual case where single scattering of the light is studied, so DLS is suitable mainly for the regime of diffusive Brownian motion. Nevertheless, several DLS experiments⁸ have, with difficulty, established the existence of the $\sqrt{\tau}$ term in Eq. (3). The problem is the very small distance moved by a particle in a time τ_v : a very small fraction of its radius, or only a few Å. This difficulty can be overcome by the use of diffusing-wave spectroscopy. In DWS an optically dense sample is used so that a photon is scattered many (~ 10 to $> 10^4$) times inside the sample. Now the required difference of λ in the optical path length results from the sum of the displacements of a large number of particles, so the typical displacement of a single particle can be very small. Thus DWS is sensitive to motions over much smaller distances and times than conventional DLS. Below we describe two DWS experiments. In the first, the nondiffusive terms in Eq. (3) just begin to be significant. However, in the second we make accurate measurements at times much shorter than τ_v , well into the range of time over which the transition from ballistic to diffusive motion occurs.

One motivation for the first set of experiments was to resolve a conflict in the literature concerning the fundamental mechanism of the transport of light in a multiply scattering medium. Pine *et al.*⁵ found that classical diffusion theory described the propagation of the multiply scattered light so that its typical path length, and therefore the number of scatterings, increased as the square of the sample thickness L . However, Freund, Kaveh, and Rosenbluh⁹ reported a linear increase of optical path

with L and suggested a theory for the "ballistic transport" of light. Resolution of this conflict is an essential first step if DWS is to be used for quantitative measurements.

To investigate these contradictory results we use experimental parameters similar to those used in Ref. 9: aqueous suspensions of polystyrene spheres with $a = 0.206 \mu\text{m}$ and volume fraction $\phi = 0.1$, contained in flat sample cells with L ranging from 0.1 to 2 mm. The beam from a Kr^+ -ion laser was focused onto one face of the sample. Multiply scattered light, transmitted through the other face, was imaged (1:1) on a 200- μm circular aperture and detected through a second aperture placed ~ 30 cm behind the first. Several different laser wavelengths were used. We measured the intensity correlation function directly in the time domain, using a photon correlator. Spurious effects introduced at small delay times ($\tau \leq 1 \mu\text{sec}$) by electronic distortions and after pulsing of the photomultiplier tubes were minimized by splitting the light emerging from the detector aperture equally into two separate photomultiplier tubes whose outputs were cross correlated.¹⁰ The signal entering the shift register of the correlator was delayed by about 1 μsec by passing it through a long cable. With a correlator sample time of 0.05 μsec , this procedure provides reliable measurements of intensity correlation functions with decay times as short as 0.3 μsec at both positive and negative values of delay time τ (see inset, Fig. 1). Normalized field correlation functions $g_1(\tau)$ were obtained from the measured normalized intensity correlation functions $g_2(\tau)$ through the relation $g_2(\tau) = 1 + \beta[g_1(\tau)]^2$, where β is a factor (< 1) determined largely by the size of the detection aperture. Experiments were performed at room temperature, $\sim 20^\circ\text{C}$.

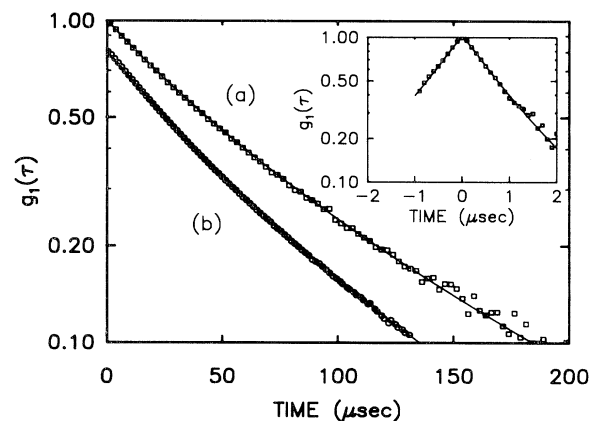


FIG. 1. Plots of $\ln g_1(\tau)$ vs delay times τ : Curve *a*, polystyrene spheres of radius $0.206 \mu\text{m}$ in water, wavelength $\lambda = 530.9 \text{ nm}$, cell thickness $L = 0.2 \text{ mm}$. Curve *b*, PMMA spheres of radius $0.50 \mu\text{m}$ in hexane, $\lambda = 530.9 \text{ nm}$, $L = 1 \text{ mm}$ (offset for clarity). Inset: Same as for curve *a* except $L = 2 \text{ mm}$. Solid lines are theory calculated from Eqs. (3) and (4); note the good agreement.

An example of a typical field correlation function is shown in Fig. 1(a) for $L=0.2$ mm and $\lambda=530.9$ nm. The inset of Fig. 1 shows the much more rapid decay obtained from a sample 10 times thicker, $L=2$ mm. Both correlation functions exhibit apparently well-defined initial decays, linear regions in the semilogarithmic plots. We measure the first cumulants,

$$\Gamma_1 = -\lim_{\tau \rightarrow 0} \frac{d}{dt} \ln g_1(\tau),$$

by graphical analysis of the data and plot these as a function of L for three different values of λ in Fig. 2.

To analyze these results we assume that the transport of light through the sample is diffusive with a transport mean free path l^* .¹¹ An expression for the field correlation function is obtained by solving the diffusion equation with boundary conditions which ensure that the flux of diffusing photons goes to zero a distance l^* outside the faces of the sample.⁶ For the experimental geometry used we obtain

$$g_1(\tau) \propto \int_{(L/l^*)}^{\infty} [2k^2 \langle \Delta x^2(\tau) \rangle]^{1/2} [A(s) \sinhs + e^{-s(1-\epsilon)}] ds, \quad (4a)$$

where

$$A(s) = \frac{(\epsilon s - 1)[\epsilon s e^{-\epsilon} + (\sinhs + \epsilon s \coshs) e^{-s(1-\epsilon)}]}{(\sinhs + \epsilon s \coshs)^2 - (\epsilon s)^2}, \quad (4b)$$

$\epsilon = 2l^*/3L$, and $k = 2\pi n/\lambda$, with n the index of refraction of water.

If we assume $\langle \Delta x^2(\tau) \rangle$ in Eq. (4) to have its asymptotic form, $2D\tau$, it can be shown from Eq. (4) that $\Gamma_1 \propto L^2$ for $L/l^* \gg 1$, as expected for diffusive transport. The

dependences of Γ_1 on L seen in Fig. 2 are certainly much closer to this quadratic prediction of the photon diffusion assumption than to the linear dependence found by Freund, Kaveh, and Rosenbluh.⁹ Nevertheless, some downward curvature is observed at short wavelengths and large thicknesses when Γ_1 is large and $g_1(\tau)$ decays rapidly. At these short times the nondiffusive terms in Eq. (3) cannot be neglected. If the full expression of Eq. (3) is used in Eq. (4) to calculate $g_1(\tau)$, it is no longer possible to define an initial slope (see inset, Fig. 3). Initially, $\ln g_1(\tau)$ curves downward, reflecting the short-time dependence of $\langle \Delta x^2(\tau) \rangle$ or τ ; at longer times it curves upward due to the contributions from different photon path lengths s in Eq. (4). However, we can calculate from Eqs. (3) and (4) the value of $-d \ln g_1(\tau)/d\tau$ at the point of inflection, $d^2 \ln g_1(\tau)/d\tau^2 = 0$, and assume that this is equivalent to the apparent first cumulant determined graphically from the data. The results of this operation are shown as the lines in Fig. 2; agreement between experiment and theory is excellent. The only parameters fitted in this comparison are the transport mean free paths l^* . We obtain $l^* = 25.7 \mu\text{m}$ for $\lambda = 647.1$ nm, $l^* = 21.5 \mu\text{m}$ for $\lambda = 530.9$ nm, and $l^* = 14.9 \mu\text{m}$ for $\lambda = 406.1$ nm, which compare favorably with the values 22.2, 20.3, and 16.2 μm , respectively, calculated from Mie scattering theory.

From this set of measurements we conclude the following: (i) the transport of the photons is diffusive; we find no evidence for the ballistic transport of photons suggested by Freund, Kaveh, and Rosenbluh.⁹ (ii) The short-time motion of the Brownian particles is not diffusive and is readily accessed by DWS.

To study this nondiffusive Brownian motion in greater detail, we can increase τ_v and thus extend the non-

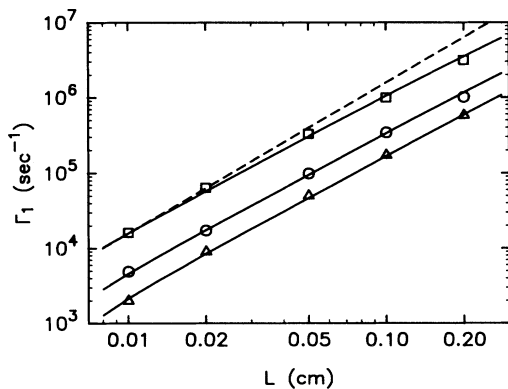


FIG. 2. Apparent first cumulants Γ_1 for polystyrene samples as functions of cell thickness L and wavelength λ (Δ , 647.1 nm; O , 530.9 nm; \square , 406.1 nm), determined by graphical analysis of correlation functions $g_1(\tau)$. Solid lines are $-d \ln g_1(\tau)/d\tau$ at τ such that $d^2 \ln g_1(\tau)/d\tau^2 = 0$, where $g_1(\tau)$ is calculated from Eqs. (3) and (4). The dashed line is simple photon diffusion theory, $\Gamma_1 \propto L^2$.

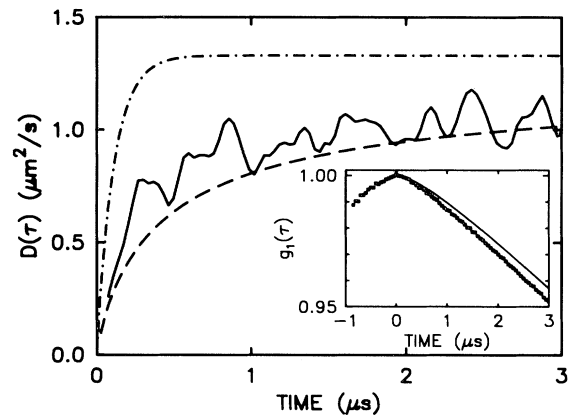


FIG. 3. Main plot: Time-dependent diffusion coefficient determined from the slope of $g_1(\tau)$ for small τ . Solid line, experiment; dash-dotted line, exponential theory [Eq. (2)]; dashed line, hydrodynamic theory [Eq. (3)]. Inset: $g_1(\tau)$ measured for the PMMA sample with correlator sample time 0.05 μsec ; solid line is $g_1(\tau)$ calculated from Eqs. (3) and (4).

diffusive regime to longer times. This is accomplished by using spheres of polymethylmethacrylate (PMMA) with radius $a=0.5\ \mu\text{m}$, $\phi\approx 0.15$, and suspended in hexane which has $\rho=0.659\ \text{g/cm}^3$ and $\eta=0.326\ \text{cP}$. For this system, $\tau_v=0.51\ \mu\text{sec}$ to be compared with $0.042\ \mu\text{sec}$ for the polystyrene system. Figure 1(b) shows the field correlation function obtained from the PMMA sample in a cell of thickness $L=1\ \text{mm}$ with light of wavelength $\lambda=530.9\ \text{nm}$. Although the overall shape is similar to that of the polystyrene spheres shown in the same figure, a slight downward curvature at the shortest delay times is evident, reflecting nondiffusive behavior of $\langle\Delta x^2(\tau)\rangle$. Accordingly in the inset of Fig. 3 we show a measurement made with correlator sample time $0.05\ \mu\text{sec}$, 30 times smaller than in Fig. 1(b). Now the downward curvature is marked and the initial slope of $\ln g_1(\tau)$ is close to zero. Note that here $g_1(\tau)$ decays by only 5% and that the shortest delay time corresponds to $\tau\approx\tau_v/10$. The solid line in Fig. 1(b) is a fit by Eqs. (3) and (4) with only l^* as an adjustable parameter; this gives $l^*=112\ \mu\text{m}$, to be compared with the calculated value of $122\ \mu\text{m}$. These longer-time-delay data are relatively insensitive to the effects of the nondiffusive motion, thus providing a reliable measure of l^* . The solid line in the inset of Fig. 3 is calculated from Eqs. (3) and (4) using this fitted value of l^* . While experiment and theory show the same trends, slight differences are apparent. An alternative way of presenting the data follows from recognizing that, for small τ , Eq. (4) can be expanded to become $g_1(\tau)=1-B(L/l^*)^2k^2\langle\Delta x^2(\tau)\rangle$, where B depends weakly on L/l^* ; here $B=0.425$. Thus the mean-square displacement $\langle\Delta x^2(\tau)\rangle$ can be calculated directly from Fig. 3. We define a time-dependent diffusion coefficient⁸ by $D(\tau)=\frac{1}{2}d\langle\Delta x^2(\tau)\rangle/d\tau [= \int_0^\tau R(t)dt]$ and estimate it by numerical differentiation of the data. The results are shown in Fig. 3, compared with the predictions of the exponential and hydrodynamic theories [Eqs. (2) and (3)]. Again the data follow the trend of the hydrodynamic theory, although with some differences apparent. Note that the smallest measured value of $D(\tau)$ is $\sim 0.2D$ so that the experiment probes well into the transition from ballistic to diffusive motion.

The analyses given above of both experiments have assumed that interactions between particles can be neglected. At volume fractions of 0.1 and 0.15 this is certainly too simple an assumption. Inclusion of interactions will lead to significant theoretical complications. Firstly, a single scattering event will probe collective motions of a group of particles. Secondly, the diffusive photon paths

will be determined not only by the particle's form factor but also by the suspension's structure factor.¹² Interaction effects may well be the cause of the disagreement between experiment and theory found in the PMMA measurements. A full theory must also include time-dependent hydrodynamic interactions¹³ between different particles as well as the "self-hydrodynamic interaction" expressed by Eq. (3).

In conclusion, we have verified that the transport of light in a multiply scattering medium is diffusive and have used DWS to quantitatively study new physics at very short length scales by probing the transition at short times from ballistic to diffusive motion of a Brownian particle. In future work we intend to make a detailed test of Eq. (3) by using a more dilute PMMA sample and to attempt to investigate time-dependent interparticle hydrodynamic interactions in concentrated samples.

We thank R. H. Ottewill and D. M. Metcalfe for providing the PMMA sample.

-
- ¹E. J. Hinch, *J. Fluid Mech.* **72**, 499 (1975).
²B. J. Alder and T. E. Wainwright, *Phys. Rev. Lett.* **18**, 988 (1967); *Phys. Rev. A* **1**, 18 (1970).
³G. Maret and P. E. Wolf, *Z. Phys. B* **65**, 409 (1987).
⁴M. J. Stephen, *Phys. Rev. B* **37**, 1 (1988).
⁵D. J. Pine, D. A. Weitz, P. M. Chaikin, and E. Herbolzheimer, *Phys. Rev. Lett.* **60**, 1134 (1988).
⁶D. J. Pine, D. A. Weitz, G. Maret, P. E. Wolf, E. Herbolzheimer, and P. M. Chaikin, in *Scattering and Localization of Classical Waves in Random Media*, edited by P. Sheng (World Scientific, Singapore, 1989).
⁷See, for example, B. J. Berne and R. Pecora, *Dynamic Light Scattering* (Wiley, New York, 1976).
⁸A. Boullier, J.-P. Boon, and P. Deguent, *J. Phys. (Paris)* **39**, 159 (1978); G. L. Paul and P. N. Pusey, *J. Phys. A* **14**, 3301 (1981); K. Ohbayashi, T. Kohno, and H. Utiyama, *Phys. Rev. A* **27**, 2636 (1983).
⁹I. Freund, M. Kaveh, and M. Rosenbluh, *Phys. Rev. Lett.* **60**, 1130 (1988).
¹⁰H. C. Burstyn and J. V. Sengers, *Phys. Rev. A* **27**, 1071 (1983); B. Hinz, G. Simonsohn, M. Hendrix, G. Wu, and A. Leipertz, *J. Mod. Opt.* **34**, 1093 (1987).
¹¹A. Ishimaru, *Wave Propagation and Scattering in Random Media: Single Scattering and Transport Theory* (Academic, New York, 1978), Vol. 1.
¹²F. C. MacKintosh and S. John, *Phys. Rev. B* **40**, 2383 (1989).
¹³W. Van Saarloos and P. Mazur, *Physica (Amsterdam)* **120A**, 77 (1983).